

Numerical Dissipation and Wrong Propagation Speed of Discontinuities For Stiff Source Terms

H.C. Yee^a, D.V. Kotov^b, B. Sjögren^c

^aNASA-Ames Research Center, Moffett Field, CA, 94035, USA, Helen.M.Yee@nasa.gov, (650)604-4769, FAX (650)604-4377

^bPostdoctoral Fellow, Center for Turbulence Research, Stanford University, CA, 94305 USA

^cLawrence Livermore National Laboratory, Livermore, CA, 94551, USA

Abstract

In compressible turbulent combustion/nonequilibrium flows, the constructions of numerical schemes for (a) stable and accurate simulation of turbulence with strong shocks, and (b) obtaining correct propagation speed of discontinuities for stiff reacting terms on “coarse grids” share one important ingredient - minimization of numerical dissipation while maintaining numerical stability. Here “coarse grids” means standard mesh density requirement for accurate simulation of typical non-reacting flows. This dual requirement to achieve both numerical stability and accuracy with zero or minimal use of numerical dissipation is most often conflicting for existing schemes that were designed for non-reacting flows. The goal of this paper is to relate numerical dissipations that are inherited in a selected set of high order shock-capturing schemes with the onset of wrong propagation speed of discontinuities for two representative stiff detonation wave problems.

Key words: High order numerical methods, Numerical methods for turbulence with shocks, Stiff source terms, Wrong propagation speed of discontinuities

1. Introduction

To make accurate predictions in compressible (magnetized) turbulent combustion/nonequilibrium flows, one has to deal with the equations that describe time-dependent non-equilibrium effects, combustion, advanced thermodynamic models, and magnetic fields (MHD). Numerical simulation is challenging because of the conflicting requirements for numerical methods to be accurate enough to resolve the small scales of turbulence but robust enough to handle shock waves without generating spurious numerical noise. In addition, the different physics models have different time scales that, when underresolved, might interact numerically to produce erroneous results. Furthermore, the appearance of the source terms in modeling flow problems containing finite-rate chemistry or combustion poses additional numerical difficulties beyond that for solving non-reacting turbulent flows. The so-called stiff source term problem [7] is a well-known example. For stiff reactions it is well known that the wrong propagation speed of discontinuities occurs due to the

under-resolved numerical solutions in both space and time. Schemes to improve the wrong propagation speed of discontinuities for systems of stiff reacting flows remain a challenge for algorithm development [15].

In addition to the minimization of numerical dissipation while maintaining numerical stability in compressible turbulence with strong shocks, Yee & Sjögren and Yee & Sweby [19, 20, 16] discussed a general framework for the design of such schemes. Yee & Sjögren [22], Wang et al. [15] and references cited therein present their recent progress on the subject. In [25] a short overview of this recent progress is given. Two very important numerical challenges are “Stiffness and Nonlinearity of Source Terms”.

The objective of the present paper is to gain a deeper understanding on the behavior of four high order shock-capturing schemes with the onset of wrong propagation speed of discontinuities for two representative stiff detonation wave problems. The test cases consist of the Arrhenius 1D Chapman-Jouguet (C-J) detonation wave [4, 13] and a 2D Heaviside detonation wave [1]. These are the same two test cases considered in [15]. The considered four schemes are the fifth-order WENO, “WENO5”, the newly developed subcell resolution version of WENO5, “WENO5/SR” [15], the Yee & Sjögren nonlinear filter version of WENO5 using a local flow sensor to further limit the amount of WENO5 numerical dissipation, “WENO5fi”, and the Ducros split version of WENO5fi, “WENO5fi+split” [21, 22]. All of the four methods use the Roe’s average states. For the temporal discretization the classical fourth-order Runge-Kutta method (RK4) is used. See the aforementioned references for the development of these schemes.

WENO5/SR [15] is a newly developed modified fractional step method which solves the convection step and reaction step separately. In the convection step any high order shock-capturing method can be used. In the reaction step an ODE solver is applied, but with the computed flow variables in the shock region modified by the Harten subcell resolution idea [3].

WENO5fi is the filter version of WENO5. On the first stage a full time step by RK4 is performed. For this stage the sixth-order central spatial base scheme is used. On the second stage the solution is filtered by the dissipative portion of WENO5 in conjunction with a local wavelet flow sensor [22]. The wavelet flow sensor indicates the locations and the amount where shock-capturing dissipations are needed and leaves the remaining region free of numerical dissipation contamination. WENO5fi+split is WENO5fi applied to the Ducros et al. split form of the governing equation [2] before the application of WENO5fi. The Ducros et al. split form is a preprocessing step to condition the governing equation(s) before the application of high order central schemes. This preprocessing step improves numerical stability and is widely used in numerical modeling and simulation of turbulent flows.

The comparison of the performance of the four schemes is largely based on the degree that each method captures the correct location and jump size of the stiff reaction front for coarse grids. Here “coarse grids” means standard mesh density requirement for accurate simulation of typical non-reacting flows. It is remarked that, in order to resolve the sharp

reaction zone, sufficiently many grid points in this zone are still needed. The behavior of these schemes in the vicinity of a sharp reaction zone with several levels of grid refinement will be briefly touched upon.

2. Numerical methods

Consider a 2D reactive Euler equation with two chemical states of burnt gas and unburnt gas and a single irreversible reaction. Without heat conduction and viscosity, the system can be written as

$$\rho_t + (\rho u)_x + (\rho v)_y = 0 \quad (1)$$

$$(\rho u)_t + (\rho u^2 + p)_x + (\rho uv)_y = 0 \quad (2)$$

$$(\rho v)_t + (\rho uv)_x + (\rho v^2 + p)_y = 0 \quad (3)$$

$$E_t + (u(E + p))_x + (v(E + p))_y = 0 \quad (4)$$

$$(\rho z)_t + (\rho uz)_x + (\rho vz)_y = -K(T)\rho z, \quad (5)$$

where $\rho(x, y, t)$ is the mixture density, $u(x, y, t)$ and $v(x, y, t)$ are the mixture x - and y -velocities, $E(x, y, t)$ is the mixture total energy per unit volume, $p(x, y, t)$ is the pressure, $z(x, y, t)$ is the mass fraction of the unburnt gas, $K(T)$ is the chemical reaction rate and $T(x, y, t)$ is the temperature. The pressure is given by

$$p = (\gamma - 1)\left(E - \frac{1}{2}\rho(u^2 + v^2) - q_0\rho z\right), \quad (6)$$

where the temperature $T = \frac{p}{\rho}$ and q_0 is the chemical heat released in the reaction.

The reaction rate $K(T)$ is modeled by an Arrhenius law

$$K(T) = K_0 \exp\left(\frac{-T_{ign}}{T}\right), \quad (7)$$

where K_0 is the reaction rate constant and T_{ign} is the ignition temperature. The reaction rate may be also modeled in the Heaviside form

$$K(T) = \begin{cases} 1/\varepsilon & T \geq T_{ign} \\ 0 & T < T_{ign} \end{cases}, \quad (8)$$

where ε is the reaction time and $1/\varepsilon$ is roughly equal to K_0 .

Here only the newly developed high order finite difference method with subcell resolution for advection equations with stiff source terms [15] in 2D is briefly summarized. The key aspect of the filter counterpart of the WENO schemes are included at the end of the section.

2.1. *High order finite difference methods with subcell resolution for advection equations with stiff source terms*

The general fractional step approach based on Strang-splitting [12] for equation

$$U_t + F(U)_x + G(U)_y = S(U) \quad (9)$$

is as follows. The numerical solution at time level t_{n+1} is approximated by

$$U^{n+1} = A \left(\frac{\Delta t}{2} \right) R(\Delta t) A \left(\frac{\Delta t}{2} \right) U^n. \quad (10)$$

The reaction operator R is over a time step Δt and the convection operator A is over $\Delta t/2$. The two half-step reaction operations over adjacent time steps can be combined to save cost. The convection operator A is defined to approximate the solution of the homogeneous part of the problem on the time interval, i.e.,

$$U_t + F(U)_x + G(U)_y = 0, \quad t_n \leq t \leq t_{n+1}. \quad (11)$$

The reaction operator R is defined to approximate the solution on a time step of the reaction problem:

$$\frac{dU}{dt} = S(U), \quad t_n \leq t \leq t_{n+1}. \quad (12)$$

Here, the convection operator consists of, e.g., WENO5 with Roe flux and RK4 for time discretization. If there is no smearing of discontinuities in the convection step, any ODE solver can be used as the reaction operator. However, all the standard shock-capturing schemes will produce a few transition points in the shock when solving the convection equation. These transition points are usually responsible for causing incorrect numerical results in the stiff case. Thus we cannot directly apply a standard ODE solver at these transition points. Here the Harten's subcell resolution technique in the reaction step is employed. The general idea is as follows. If a point is considered a transition point of the shock, information from its neighboring points which are deemed not transition points will be used instead. In 2D case we apply the subcell resolution procedure dimension by dimension. Here, $U^T = (\rho, \rho u, \rho v, E, \rho z)$. The algorithm proceeds as follows.

(1) Use a ‘‘shock indicator’’ to identify cells in which discontinuities are believed to be situated. One can use any indicator suitable for the particular problem. Here the minmod-based shock indicator in [3, 11] is considered. Identify troubled cell I_{ij} in both x - and y -directions by applying the shock indicator to, e.g., the mass fraction z . Define the cell I_{ij} as troubled in the x -direction if $|s_{ij}^x| \geq |s_{i-1,j}^x|$ and $|s_{ij}^x| \geq |s_{i+1,j}^x|$ with at least one strict inequality, where

$$s_{ij}^x = \text{minmod}\{z_{i+1,j} - z_{ij}, z_{ij} - z_{i-1,j}\}. \quad (13)$$

Similarly we can define the cell I_{ij} as troubled in the y -direction if $|s_{ij}^y| \geq |s_{i,j-1}^y|$ and $|s_{ij}^y| \geq |s_{i,j+1}^y|$ with at least one strict inequality where

$$s_{ij}^y = \text{minmod}\{z_{i,j+1} - z_{ij}, z_{ij} - z_{i,j-1}\}. \quad (14)$$

If I_{ij} is only troubled in one direction, we apply the subcell resolution along this direction. If I_{ij} is troubled in both directions, we choose the direction which has a larger jump. Namely, if $|s_{ij}^x| \geq |s_{ij}^y|$, subcell resolution is applied along the x -direction, otherwise it is done along the y -direction. In the following steps (2)-(3), without loss of generality, we assume the subcell resolution is applied in the x -direction. Assuming I_{ij} is troubled in the x -direction, we apply subcell resolution along the x -direction.

In a troubled cell identified above, we continue to identify its neighboring cells. For example, we can define $I_{i+1,j}$ as troubled if $|s_{i+1,j}^x| \geq |s_{i-1,j}^x|$ and $|s_{i+1,j}^x| \geq |s_{i+2,j}^x|$ and similarly define $I_{i-1,j}$ as troubled if $|s_{i-1,j}^x| \geq |s_{i-2,j}^x|$ and $|s_{i-1,j}^x| \geq |s_{i+1,j}^x|$. If the cell $I_{i-s,j}$ and the cell $I_{i+r,j}$ ($s, r > 0$) are the first good cells from the left and the right (i.e., $I_{i-s+1,j}$ and $I_{i+r-1,j}$ are still troubled cells), we compute the fifth-order ENO interpolation polynomials $p_{i-s,j}(x)$ and $p_{i+r,j}(x)$ for the cells $I_{i-s,j}$ and $I_{i+r,j}$, respectively.

(2) Modify the point values z_{ij} , T_{ij} and ρ_{ij} in the troubled cell I_{ij} by the ENO interpolation polynomials

$$\begin{cases} \tilde{z}_{ij} = p_{i-s,j}(x_i; z), & \tilde{T}_{ij} = p_{i-s,j}(x_i; T), & \tilde{\rho}_{ij} = p_{i-s,j}(x_i; \rho), & \text{if } \theta \geq x_i \\ \tilde{z}_{ij} = p_{i+r,j}(x_i; z), & \tilde{T}_{ij} = p_{i+r,j}(x_i; T), & \tilde{\rho}_{ij} = p_{i+r,j}(x_i; \rho), & \text{if } \theta < x_i \end{cases}, \quad (15)$$

where the location θ is determined by the conservation of energy E

$$\int_{x_{i-1/2}}^{\theta} p_{i-s,j}(x; E) dx + \int_{\theta}^{x_{i+1/2}} p_{i+r,j}(x; E) dx = E_{ij} \Delta x. \quad (16)$$

Under certain conditions, it can be shown that there is a unique θ satisfying Eq. (16), which can be solved using, for example, a Newton's method. If there is no solution for θ or there is more than one solution, we choose $\tilde{z}_{ij} = z_{i+r,j}$, $\tilde{T}_{ij} = T_{i+r,j}$ and $\tilde{\rho}_{ij} = \rho_{i+r,j}$. For particular problems one can choose any other suitable method for the reconstruction.

(3) Use \tilde{U}_{ij} instead of U_{ij} in the ODE solver if the cell I_{ij} is a troubled cell. For simplicity, explicit Euler is used as the ODE solver.

$$(\rho z)_{ij}^{n+1} = (\rho z)_{ij}^n + \Delta t S(\tilde{T}_{ij}, \tilde{\rho}_{ij}, \tilde{z}_{ij}). \quad (17)$$

In general, a regular CFL=0.1 can be used in the proposed scheme to produce a stable solution. But the solution is very coarse in the reaction zone because of the underresolved mesh in time. In order to obtain more accurate results in the reaction zone, we evolve one reaction step via N_r sub steps, i.e.,

$$u^{n+1} = A \left(\frac{\Delta t}{2} \right) R \left(\frac{\Delta t}{N_r} \right) \cdots R \left(\frac{\Delta t}{N_r} \right) A \left(\frac{\Delta t}{2} \right) u^n \quad (18)$$

in some numerical examples studied in [15].

2.2. Well-Balanced High Order Filter Schemes for Reacting Flows [9, 21, 22, 24]

Before the application of a high order non-dissipative spatial base scheme, the pre-processing step to improve stability had split inviscid flux derivatives of the governing equation(s) in the following three ways, depending on the flow types and the desire for rigorous mathematical analysis or physical argument.

- Entropy splitting of Olsson & Olinger [8] and Yee et al. [18, 19]: The resulting form is non-conservative and the derivation is based on entropy norm stability with numerical boundary closure for the initial value boundary problem.
- The system form of the Ducros et al. splitting [2]: This is a conservative splitting and the derivation is based on physical arguments.
- Tadmor entropy conservation formulation for systems (Sjögreen & Yee [10]): The derivation is based on mathematical analysis. It is a generalization of Tadmor's entropy formulation to systems and has not been fully tested on complex flows.

After the application of a non-dissipative high order spatial base scheme on the split form of the governing equation(s), to further improve nonlinear stability from the non-dissipative spatial base scheme, the post-processing step of Yee & Sjögreen [21, 22], Sjögreen & Yee [9] nonlinearly filtered the solution by a dissipative portion of a high order shock-capturing scheme with a local flow sensor. The flow sensor provides locations and amounts of built-in shock-capturing dissipation that can be further reduced or eliminated. The idea of these nonlinear filter schemes for turbulence with shocks is that, instead of solely relying on very high order high-resolution shock-capturing methods for accuracy, the filter schemes [17, 18, 9, 21] take advantage of the effectiveness of the nonlinear dissipation contained in good shock-capturing schemes as stabilizing mechanisms (a post-processing step) at locations where needed. The nonlinear dissipative portion of a high-resolution shock-capturing scheme can be any shock-capturing scheme. By design, the flow sensors, spatial base schemes and nonlinear dissipation models are standalone modules. Unlike standard shock-capturing and/or hybrid shock-capturing methods, the nonlinear filter method requires one Riemann solve per dimension per time step, independent of time discretizations. The nonlinear filter method is more efficient than its shock-capturing method counterparts employing the same order of the respective methods. See [22, 24] for the recent improvements of the work [17, 18, 9, 21] that are suitable for a wide range of flow speed with minimal tuning of scheme parameters. For all the computations shown, the Ducros et al. splitting is employed. This is due to the fact that for the subject test cases we need a robust conservative splitting as the preprocessing step. The subcell resolution approach using the fractional step procedure can carry over to the aforementioned filter schemes as well. Some attributes of the high order filter approach are:

- Spatial Base Scheme: High order and conservative (no flux limiter or Riemann solver)

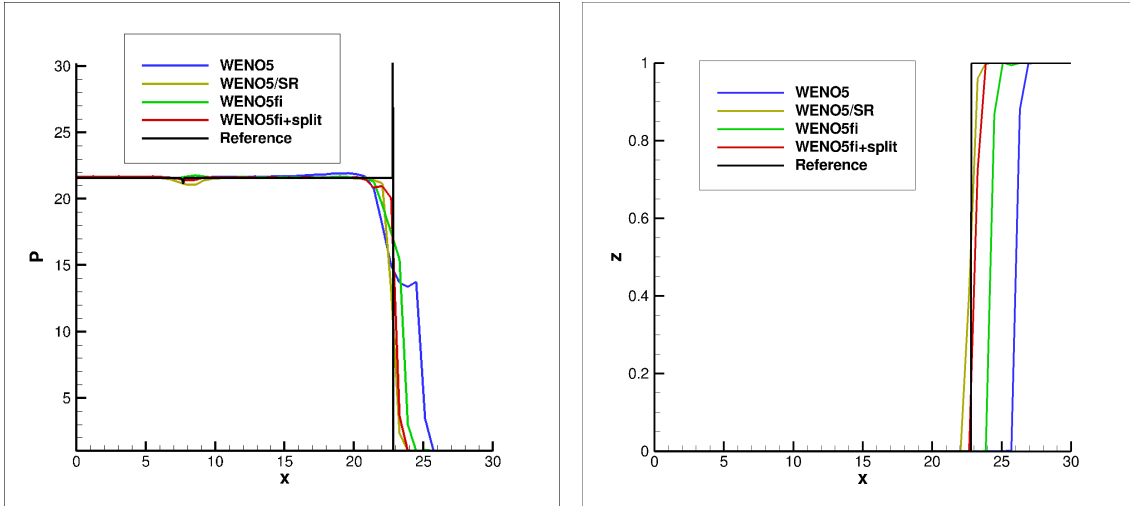


Figure 1: Pressure and density (mass fraction of unburnt gas) comparison among four high order shock-capturing methods for the C-J detonation problem, Arrhenius case at $t = 1.8$ using 50 uniform grid points.

- **Physical Viscosity:** Contribution of physical viscosity, if it exists, is automatically taken into consideration by the base scheme in order to minimize the amount of numerical dissipation to be used by the filter step
- **Efficiency:** One Riemann solve per dimension per time step, independent of time discretizations (less CPU time and fewer grid points than their standard shock-capturing scheme counterparts)
- **Accuracy:** Containment of numerical dissipation via a local wavelet flow sensor
- **Well-balanced scheme:** These nonlinear filter schemes are well-balanced schemes for certain chemical reacting flows [14]
- **Stiff Combustion with Discontinuities:** For some stiff reacting flow test cases the high order filter scheme is able to obtain the correct propagation speed of discontinuities, whereas the standard high order shock-capturing (e.g., WENO) schemes cannot (see the result below)
- **Parallel Algorithm:** Suitable for most current supercomputer architectures

3. Numerical Examples

The behavior of the considered four methods is investigated on two test cases that were considered in [15]. The test cases consist of the Arrhenius 1D C-J detonation wave and a 2D Heaviside detonation wave. Note that the computed solutions by WENO5 and WENO5/SR presented here could be slightly different from the results presented in [15] due to the minor

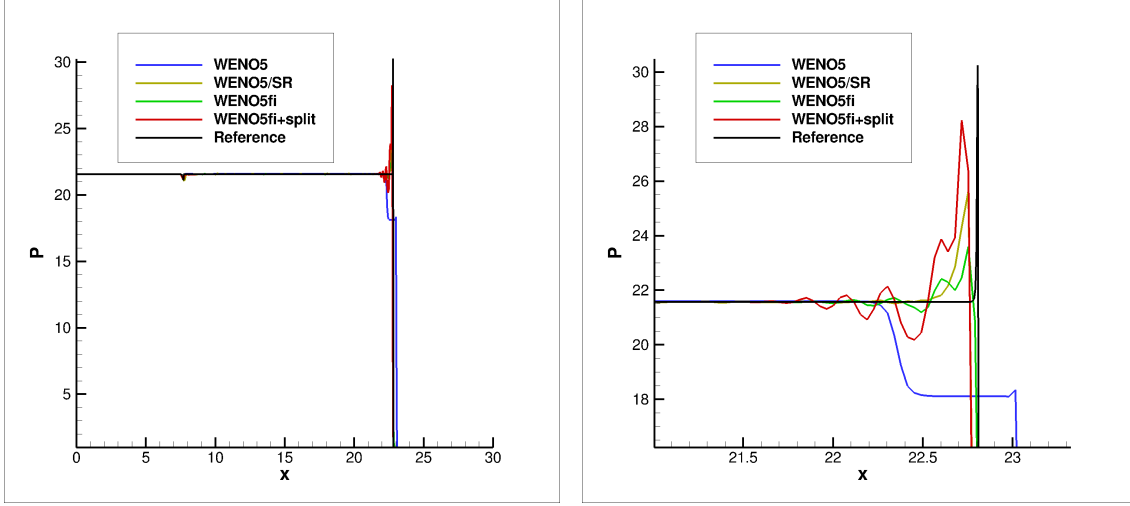


Figure 2: Pressure comparison among four high order shock-capturing methods for the C-J detonation problem, Arrhenius case at $t = 1.8$ using 800 uniform grid points.

differences in the formulation of the problem (governing equation; e.g., different choice of variables) and the use of cell centered and cell-vertex formulation of numerical schemes.

3.1. Chapman-Jouguet (C-J) Detonation Wave (Arrhenius Case)

The test case is the 1D C-J detonation wave (Arrhenius case) [4, 13]. The initial values consist of totally burnt gas on the left-hand side and totally unburnt gas on the right-hand side. The density, velocity, and pressure of the unburnt gas are given by $\rho_u = 1$, $u_u = 0$ and $p_u = 1$.

The initial state of the burnt gas is calculated from C-J condition:

$$p_b = -b + (b^2 - c)^{1/2}, \quad (19)$$

$$\rho_b = \frac{\rho_u [p_b(\gamma + 1) - p_u]}{\gamma p_b}, \quad (20)$$

$$S_{CJ} = [\rho_u u_u + (\gamma p_b \rho_b)^{1/2}] / \rho_u, \quad (21)$$

$$u_b = S_{CJ} - (\gamma p_b / \tau h o_b)^{1/2}, \quad (22)$$

where

$$b = -p_u - \rho_u q_0 (\gamma - 1), \quad (23)$$

$$c = p_u^2 + 2(\gamma - 1)p_u \rho_u q_0 / (\gamma + 1). \quad (24)$$

The heat release $q_0 = 25$ and the ratio of specific heats is set to $\gamma = 1.4$. The ignition temperature $T_{ign} = 25$ and $K_0 = 164180$. The computation domain is $[0, 30]$. Initially, the discontinuity is located at $x = 10$. At time $t = 1.8$, the detonation wave has moved to $x = 22.8$. The reference solution is computed by the regular WENO5

scheme with 10000 uniform grid points and CFL=0.05. Figure 1 shows the pressure and mass fraction comparison among the standard WENO5 scheme, WENO5/SR, WENO5fi and WENO5fi+split using 50 uniform grid points. For this particular problem and grid size, WENO5fi+split compares well with WENO5/SR for the computed pressure solution. WENO5/SR and WENO5fi+split can capture the correct structure using fewer grid points than those in Helzel et al. and Tosatto & Vigevano [4, 13]. A careful examination of the 50 coarse grid mass fraction solutions indicates that WENO5fi+split is one grid point ahead of WENO5/SR at the discontinuity location when compared to the reference solution. The reference solution is obtained by WENO5 using 10,000 grid points. Since WENO5fi+split is less dissipative than WENO5, the restriction of the shock-capturing dissipation using the wavelet flow sensor helps to improve the wrong propagation speed of discontinuities without the subcell resolution procedure. Figure 2 shows a grid refinement in the hope of resolving the narrow reaction zone using 800 uniform grid points. It is interesting to see that all of the methods (except WENO5) produce oscillatory solutions in the vicinity of the reaction front. This behavior prompted us to perform a systematic six levels of uniform grid refinements (200, 400, 800, 1600, 3200 and 6400). As the number of grid point increases, this oscillatory behavior in the vicinity of the reaction front becomes more pronounced. It appears that for this particular test case the new subcell resolution scheme WENO5/SR, WENO5fi and WENO5fi+split only perform well with coarse grids. However, for the more dissipative scheme WENO5, as we refine the grid, the computed solution gets closer and closer to the reference solution.

3.2. 2D detonation waves

This example is taken from [1]. The chemical reaction is modeled by the Heaviside form with the parameters

$$\gamma = 1.4, \quad q_0 = 0.5196 \times 10^{10}, \quad \frac{1}{\varepsilon} = 0.5825 \times 10^{10}, \quad T_{ign} = 0.1155 \times 10^{10}$$

in CGS units. Consider a two-dimensional channel of width 0.005 with solid walls at the upper and lower boundaries. The computational domain is $[0, 0.025] \times [0, 0.005]$. The initial conditions are

$$(\rho, u, v, p, z) = \begin{cases} (\rho_b, u_b, 0, p_b, 0), & \text{if } x \leq \xi(y), \\ (\rho_u, u_u, 0, p_u, 1), & \text{if } x > \xi(y), \end{cases} \quad (25)$$

where

$$\xi(y) = \begin{cases} 0.004 & |y - 0.0025| \geq 0.001, \\ 0.005 - |y - 0.0025| & |y - 0.0025| < 0.001, \end{cases} \quad (26)$$

and $u_u = 0$, $\rho_u = 1.201 \times 10^{-3}$, $p_u = 8.321 \times 10^5$ and $u_b = 8.162 \times 10^4$. Values of p_b and ρ_b are defined by Eq. (19) and (20). In this case u_b is greater than defined by Eq. (22).

One important feature of this solution is the appearance of triple points, which travel in the transverse direction and reflect from the upper and lower walls. A discussion of the mechanisms driving this solution is given in [6]. Figures 3 and 4 show the density comparison among the standard WENO5 scheme, WENO5/SR and WENO5fi+split using

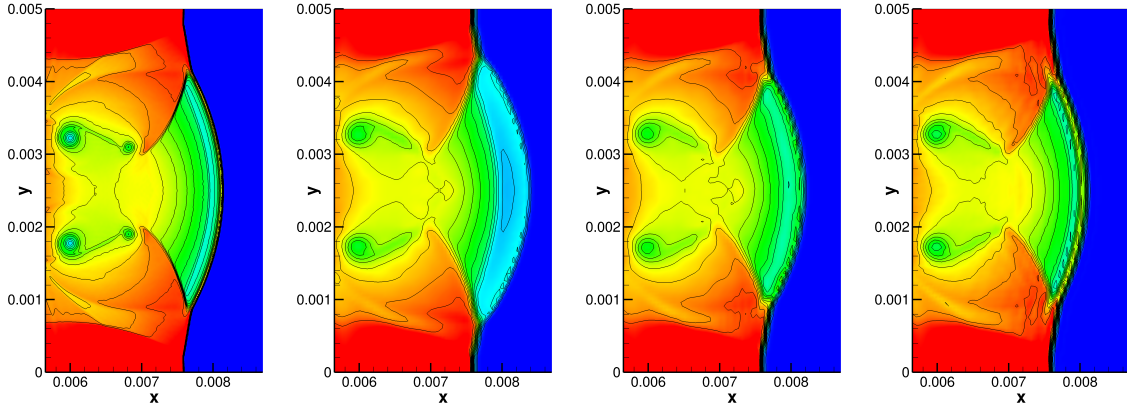


Figure 3: Density computed for the 2D detonation problem at $t = 0.3 \times 10^{-7}$ by different methods. From left to right: reference solution by the standard WENO5 method using 2000×400 uniform grid points, WENO5, WENO5/SR and WENO5fi+split using 500×100 uniform grid points.

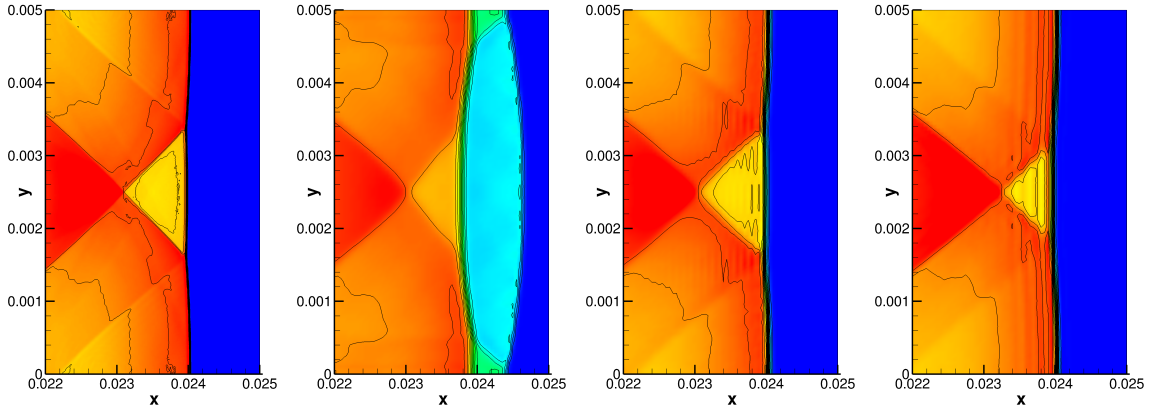


Figure 4: Density computed for the 2D detonation problem at $t = 1.7 \times 10^{-7}$ by different methods. From left to right: reference solution by the standard WENO5 method using 2000×400 uniform grid points, WENO5, WENO5/SR and WENO5fi+split using 500×100 uniform grid points.

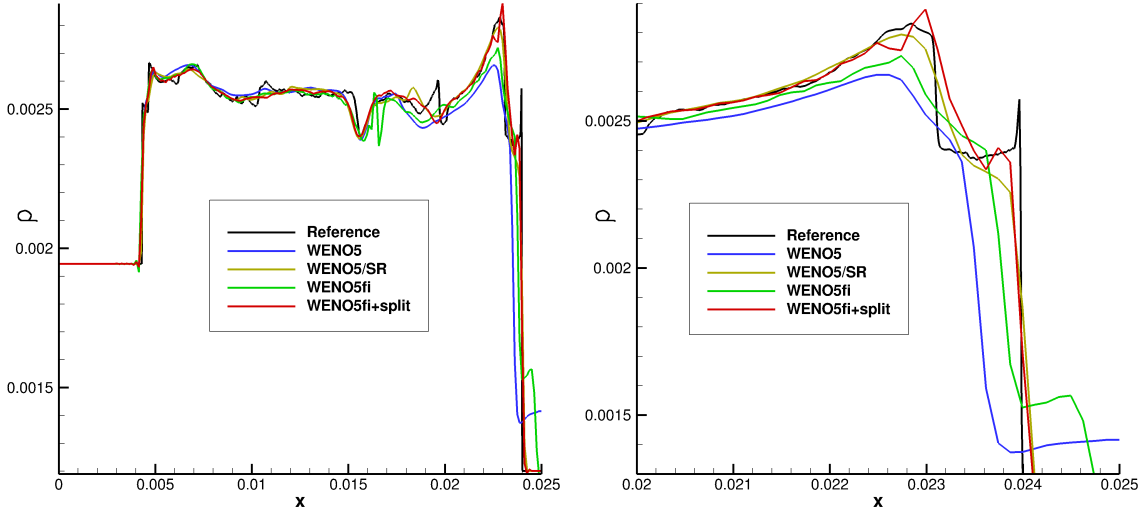


Figure 5: 1D cross-section of density at $t = 1.7 \times 10^{-7}$ by four high order shock-capturing methods for the 2D detonation problem using 200×40 uniform grid points with the left figure in the vicinity of the discontinuity.

500×100 uniform grid points at two different times. Figure 5 shows the density comparison among the standard WENO5 scheme, WENO5/SR, WENO5fi and WENO5fi+split using 200×40 and 500×100 uniform grid points. The reference solutions are computed by standard WENO5 with 2000×400 grid points. Again, WENO5/SR and WENO5fi+split are able to obtain the correct shock speed with similar accuracy. WENO5fi gives a slight oscillatory solution near $x = 0.004$. WENO5 and WENO5/SR produce no oscillations at the same location. Further improvement of the flow sensor of the filter scheme is needed in order to remove the spurious oscillations. Furthermore, for the 500×100 grid, WENO5fi also obtained the correct shock speed.

In summary, we demonstrated that the filter version of the WENO5 in conjunction with the Ducros et al. splitting (WENO5fi+split) is able to obtain the correct propagation speed of discontinuities for two detonation problems. From the result WENO5/SR and WENO5fi+split are able to obtain the correct shock speed with similar accuracy, whereas this is not the case for WENO5 WENO5fi using the same coarse grids. Using its original form [22] without further modification, the accuracy of WENO5fi+split is nearly as good as the proposed high-order finite difference schemes with subcell resolution. The next step is to examine the subcell resolution version of WENO5fi and WENO5fi+split, and their seventh-order counterparts..

Acknowledgments

The support of the DOE/SciDAC SAP grant DE-AI02-06ER25796 is acknowledged. The work was performed by the second author as a postdoc fellow at the Center for Turbulence Research, Stanford University. The financial support from the NASA Fundamental Aeronautics (Hypersonic) program for the first author is gratefully acknowledged. The

work by the third author was performed under the auspices of the U.S. Department of Energy by Lawrence Livermore National Laboratory under Contract DE-AC52-07NA27344.

References

- [1] W. Bao and S. Jin The random Projection Method for Hyperbolic Conservation Laws with Stiff Reaction Terms, *J. Comp. Phys.*, **163** (2000) 216-248.
- [2] F. Ducros, F. Laporte, T. Soulères, V. Guinot, P. Moinat, and B. Caruelle, *High-order Fluxes for Conservative Skew-Symmetric-like Schemes in Structured Meshes: Application to Compressible Flows*, *J. Comput. Phys.*, **161** (2000), 114–139.
- [3] A. Harten, *ENO Schemes with Subcell Resolution*, *J. Comput. Phys.*, **83** (1989) 148-184.
- [4] C Helzel, R LeVeque and G Warneke, *A Modified Fractional Step Method for the Accurate Approximation of Detonation Waves*, *SIAM J. Sci. Stat. Comp.*, **22** (1999) 1489-1510.
- [5] R.J. LeVeque and H.C. Yee, *A Study of Numerical Methods for Hyperbolic Conservation Laws with Stiff Source Terms*, *J. Comput. Phys.*, **86** (1990) 187-210.
- [6] K Kailasanath and E S Oran and J P Boris and T R Young Determination of Detonation Cell Size and the Role of Transverse Waves in Two-dimensional Detonations, *Combust. Flame*, **61** (1985) 199-209.
- [7] R.J. LeVeque and H.C. Yee, *A Study of Numerical Methods for Hyperbolic Conservation Laws with Stiff Source Terms*, *J. Comput. Phys.*, **86** (1990) 187-210.
- [8] P. Olsson and J. Oliger, *Energy and Maximum Norm Estimates for Nonlinear Conservation Laws*, RIACS Technical Report 94.01 (1994).
- [9] B. Sjögren and H. C. Yee, *Multiresolution Wavelet Based Adaptive Numerical Dissipation Control for Shock-Turbulence Computation*, *J. Scient. Computing*, **20** (2004), 211–255.
- [10] B. Sjögren and H.C. Yee, "On Skew-Symmetric Splitting and Entropy Conservation Schemes for the Euler Equations," Proceedings of the 8th European Conference on Numerical Mathematics & Advanced Applications (ENUMATH 2009), Uppsala University, June 29 - July 2, 2009, Uppsala, Sweden.
- [11] C.-W. Shu and S. Osher Efficient Implementation of Essentially Non-oscillatory Shock-Capturing Schemes, II, *J. Comp. Phys.*, **83** (1989) 32-78.
- [12] G. Strang, "On the Construction and Comparison of Difference Schemes, *SIAM J. Numer. Anal.*, **5** (1968) 506-517.

- [13] L. Tosatto and L. Vigevano, *Numerical Solution of Under-Resolved Detonations*, J. Comp. Phys., **227** (2008) 2317-2343.
- [14] W. Wang, H.C. Yee, B. Sjögreen, T. Magin, and C.W. Shu, *Construction of Low Dissipative High-Order Well-Balanced Filter Schemes for Nonequilibrium Flows*, J. Comput. Phys., **230** (2011), 4316-4335. (doi:10.1016/j.jcp.2010.04.033, 2010).
- [15] W. Wang, C.W. Shu, H.C. Yee and B. Sjögreen, *High Order Finite Difference Methods with Subcell Resolution for Advection Equations with Stiff Source Terms*, J. Comput. Physics, **231** (2012) 190-214.
- [16] H.C. Yee and P.K. Sweby, *Dynamics of Numerics & Spurious Behaviors in CFD Computations*, Keynote paper, 7th ISCFD Conference, Sept. 15-19, 1997, Beijing, China, RIACS Technical Report 97.06, June 1997.
- [17] H.C. Yee, N.D. Sandham, N.D., and M.J. Djomehri, *Low Dissipative High Order Shock-Capturing Methods Using Characteristic-Based Filters*, J. Comput. Phys., **150** (1999) 199-238.
- [18] H.C. Yee, M. Vinokur, and M.J. Djomehri, *Entropy Splitting and Numerical Dissipation*, J. Comput. Phys., **162** (2000) 33-81.
- [19] H.C. Yee and B. Sjögreen, *Designing Adaptive Low Dissipative High Order Schemes for Long-Time Integrations*, In Turbulent Flow Computation, (Eds. D. Drikakis & B. Geurts), Kluwer Academic Publisher (2002)
- [20] H.C. Yee, *Building Blocks for Reliable Complex Nonlinear Numerical Simulations*, In Turbulent Flow Computation, (Eds. D. Drikakis & B. Geurts), Kluwer Academic Publisher (2002).
- [21] H.C. Yee and B. Sjögreen, *Development of Low Dissipative High Order Filter Schemes for Multiscale Navier-Stokes/MHD Systems*, J. Comput. Phys., **225** (2007) 910-934.
- [22] H.C. Yee and B. Sjögreen, *High Order Filter Methods for Wide Range of Compressible Flow Speeds*, Proceedings of ICOSAHOM 09 (International Conference on Spectral and High Order Methods). June 22-26, 2009, Trondheim, Norway.
- [23] H.C. Yee, B. Sjögreen and A. Hadjadj, *Comparative Study of High Order Schemes for LES of Temporal-Evolving Mixing Layers*, Proceedings of ASTRONUM-2010, June 13-18, 2010, San Diego, Calif. Expanded version submitted to Computers & Fluids.
- [24] H.C. Yee and B. Sjögreen, *Local Flow Sensors in Controlling Numerical Dissipations for a Wide Spectrum of Flow Speed and Shock Strength*, in preparation.

- [25] H.C. Yee, B. Sjögren, C.W. Shu, W. Wang, T. Magin and A. Hadjadj, *On Numerical Methods for Hypersonic Turbulent Flows*, Proceedings of ESA 7th Aerothermodynamics Symposium, 9 - 12 May 2011 Site Oud Sint-Jan, Brugge, Belgium.